Face-Coordinated C_{60} Complexes with Carbido Pentaruthenium Cluster Cores Including a Bimetallic Platinum−Pentaruthenium Complex

Kwangyeol Lee and John R. Shapley*

Department of Chemistry, University of Illinois, Urbana, Illinois 60801

Received December 12, 1997

Interaction of $Ru_5C(CO)_{15}$ with C_{60} in refluxing chlorobenzene followed by PPh_3 or dppe (1,2-bis(diphenylphosphino)ethane) forms $Ru_5C(CO)_{11}(PPh_3)(\mu_3\text{-}\eta^2,\eta^2,\eta^2\text{-}C_{60})$ (**1**) or $Ru_5C(CO)_{10}(\mu\text{-}\eta^1,\eta^1\text{-dppe})(\mu_3\text{-}\eta^2,\eta^2,\eta^2\text{-}C_{60})$ (**2**), isolated in 19% and 14% yields, respectively, after chromatography. An analogous reaction of $Ru_5C(CO)_{15}$ with C_{60} followed by dppf (1,1′-bis(diphenylphosphino)ferrocene) initially forms both $Ru_5C(CO)_{11}(\eta^1\text{-dppf})(\mu_3\text{-}\eta^2,\eta^2,\eta^2\text{-}C_{60})$ (**3**) and $Ru_5C(CO)_{10}(\mu\text{-}\eta^1,\eta^1\text{-dppf})(\mu_3\text{-}\eta^2,\eta^2,\eta^2\text{-}C_{60})$ (**4**), but further thermolysis of **3** in refluxing chlorobenzene converts it to **4**. Direct interaction of $Ru_5C(CO)_{14}(PPh_3)$ (**5**), $Ru_5C(CO)_{13}$(dppe) (**6**), and $Ru_5C(CO)_{13}$(dppf) (**7**) with C_{60} in refluxing chlorobenzene also provides **1**, **2**, and **4** in isolated yields of 21%, 27%, and 20%, respectively. Interaction of $PtRu_5C(CO)_{16}$ or $PtRu_5C(CO)_{14}$(COD) with C_{60} followed by dppe in refluxing chlorobenzene forms $PtRu_5C(CO)_{11}(\eta^2\text{-dppe})(\mu_3\text{-}\eta^2,\eta^2,\eta^2\text{-}C_{60})$ (**8**) (7% and 23% yields, respectively). Substitution of the COD ligand in $PtRu_5C(CO)_{14}$(COD) by dppe at room temperature provides $PtRu_5C(CO)_{14}(\eta^2\text{-dppe})$ (**9**). Compound **9** does not react with C_{60} to give **8**. All new compounds have been characterized by a combination of analytical and spectroscopic methods, and the molecular structures of compounds **1**, **2**, **4**, **7**, **8**, and **9** have been determined by single-crystal X-ray diffraction studies.

Introduction

We have recently demonstrated the first examples of C_{60} binding as a cyclohexatriene-like C_{60} ligand to triangular faces of cluster frameworks, namely, $Ru_3(CO)_9(\mu_3\text{-}\eta^2,\eta^2,\eta^2\text{-}C_{60})$,[1] $Ru_5C(CO)_{11}(PPh_3)(\mu_3\text{-}\eta^2,\eta^2,\eta^2\text{-}C_{60})$ (**1**),[2] and $Ru_6C(CO)_{12}(\mu\text{-}\eta^1,\eta^1\text{-dppm})(\mu_3\text{-}\eta^2,\eta^2,\eta^2\text{-}C_{60})$.[2] In this paper we describe a larger series of face-coordinated C_{60} compounds having Ru_5C as well as $PtRu_5C$ cluster cores (see Scheme 1). In addition to details concerning **1**, we describe the preparation of $Ru_5C(CO)_{10}(\mu\text{-}\eta^1,\eta^1\text{-dppe})(\mu_3\text{-}\eta^2,\eta^2,\eta^2\text{-}C_{60})$ (**2**), $Ru_5C(CO)_{11}(\eta^1\text{-dppf})(\mu_3\text{-}\eta^2,\eta^2,\eta^2C_{60})$ (**3**), and $Ru_5C(CO)_{10}(\mu\text{-}\eta^1,\eta^1\text{-dppf})(\mu_3\text{-}\eta^2,\eta^2,\eta^2\text{-}C_{60})$ (**4**) from the interaction of $Ru_5C(CO)_{15}$[3] with C_{60} in refluxing chlorobenzene followed by dppe or dppf, respectively. We also show that direct interaction of $Ru_5C(CO)_{14}(PPh_3)$ (**5**),[3] $Ru_5C(CO)_{13}(\mu\text{-}\eta^1,\eta^1\text{-dppe})$ (**6**),[3] and $Ru_5C(CO)_{13}(\mu\text{-}\eta^1,\eta^1\text{-dppf})$ (**7**) with C_{60} in refluxing chlorobenzene provides **1**, **2**, and **4**, respectively. Furthermore, we have found that interaction of $PtRu_5C(CO)_{16}$[4] or $PtRu_5C(CO)_{14}$(COD)[4] with C_{60} followed by dppe in refluxing chlorobenzene forms $PtRu_5C(CO)_{11}(\eta^2\text{-dppe})(\mu_3\text{-}\eta^2,\eta^2,\eta^2\text{-}C_{60})$ (**8**). The new compounds have been characterized by analytical and spectroscopic methods in conjunction with X-ray crystallographic studies of the C_{60} complexes **1**, **2**, **4**, and **8** as well as the cluster derivatives **7** and $PtRu_5C(CO)_{14}(\eta^2\text{-dppe})$ (**9**).

Scheme 1

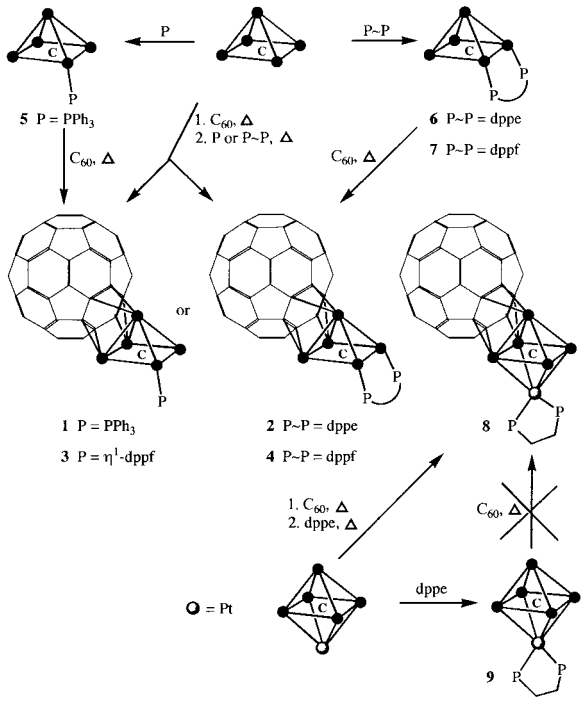

(1) Hsu, H.-F.; Shapley, J. R. *J. Am. Chem. Soc.* **1996**, *118*, 9192.
(2) Lee, K.; Hsu, H.-F.; Shapley, J. R. *Organometallics* **1997**, *16*, 3876.
(3) Johnson, B. F. G.; Lewis, J.; Nicholls, J. N.; Puga, J.; Raithby, P. R.; Rosales, M. J.; McMartin, M.; Clegg, W. *J. Chem. Soc., Dalton Trans.* **1983**, 277.
(4) Adams, R. D.; Wu, W. *J. Cluster Sci.* **1991**, *2*, 271.

S0276-7333(97)01091-1 CCC: $15.00
Publication on Web 06/17/1998

Experimental Section

All reactions were carried out under a nitrogen atmosphere by using standard inert-atmosphere techniques.[5] The reaction solvents were dried over the appropriate drying agents and distilled immediately before use: chlorobenzene (Aldrich) from CaH_2, and dichloromethane (Mallinckrodt) from CaH_2. $Ru_5C(CO)_{15}$, $Ru_5C(CO)_{14}(PPh_3)$, and $Ru_5C(CO)_{13}$(dppe) were prepared according to the literature.[3] $PtRu_5C(CO)_{16}$ and $PtRu_5C(CO)_{14}$(COD) were prepared as reported.[4] C_{60} (Southern Chemical Group), $RuCl_3 \cdot 3H_2O$ (PGM Chemicals Ltd), carbon monoxide (MG Industries), PPh_3 (Aldrich), dppe (Pressure Chemical), dppf (Aldrich), and carbon disulfide (Fisher) were used as received.

IR spectra were recorded on a Perkin-Elmer 1750 FT-IR spectrometer. ^1H, ^{13}C, and ^{31}P NMR spectra were recorded on a Varian Unity 400 spectrometer. X-ray diffraction data, negative-ion fast-atom bombardment (FAB) mass spectra using 3-nitrobenzyl alcohol as a matrix, and elemental analyses were obtained by the staff of the Materials Chemistry Laboratory, the Mass Spectrometry Center, and the Microanalytical Laboratory of the School of Chemical Sciences, respectively.

Preparation of $Ru_5C(CO)_{11}(PPh_3)(\mu_3\text{-}\eta^2,\eta^2,\eta^2\text{-}C_{60})$ (1). A. A chlorobenzene (30 mL) solution of $Ru_5C(CO)_{15}$ (40.0 mg, 0.0427 mmol) and C_{60} (33.8 mg, 0.0469 mmol) contained in a 100 mL three-neck flask equipped with a reflux condenser was heated under reflux for 1 h. During this time, the IR spectrum developed a completely new set of peaks at 2088(s), 2062(s), 2040(m, sh), and 2025(vs) cm^{-1} and the color changed from red purple to dark brown. The reaction mixture was cooled to room temperature, PPh_3 (12.3 mg, 0.0469 mmol) was added, and the reaction mixture was again heated to reflux for 5 min. The reaction mixture was cooled to room temperature, and the solvent was removed under vacuum. The dark residue was dissolved in carbon disulfide, and the solution was applied to a silica gel TLC plate, which was then eluted with carbon disulfide to give unreacted C_{60} (10.1 mg, 0.0140 mmol, 33% recovery) and **1** (14.7 mg, 0.0081 mmol, 19% based on $Ru_5C(CO)_{15}$) in order of elution. Anal. Calcd for $C_{90}H_{15}O_{11}PRu_5$: C, 59.78; H, 0.84. Found: C, 59.93; H, 0.63. Negative-ion FAB mass spectrum (^{102}Ru): *m/z* 1812 ($[Ru_5C(CO)_{11}(PPh_3)(C_{60})]^-$), 1784 ($[Ru_5C(CO)_{11}(PPh_3)(C_{60})]^- - CO$). IR ($CS_2$): ν_{CO} 2068(s), 2031(s), 2021(s), 2013(s) cm^{-1}. ^1H NMR (400 MHz, CS_2/CD_2Cl_2 (1/2), 20 °C): δ 7.70−7.55 (m, 15H). $^{31}P\{^1H\}$ NMR (162 MHz, CS_2/CD_2Cl_2 (1/2), 20 °C): δ 47.3 (s).

$Ru_5C(^{13}CO)_{11}(PPh_3)(C_{60})$ was prepared from $Ru_5C(^{13}CO)_{15}$ (ca. 95% ^{13}C). ^{13}C NMR (100 MHz, C_6H_5Cl/CD_2Cl_2 (1/2), 20 °C): δ 203.1 (s, 1C), 202.1 (s, 1C), 202.0 (s, 1C), 201.6 (s, 1C), 200.0 (s, 1C), 198.4 (s, 1C), 196.5 (s, 1C), 195.0 (s, 3C), 194.9 (s, 1C), 194.0 (s, 1C).

B. A chlorobenzene (30 mL) solution of $Ru_5C(CO)_{14}(PPh_3)$ (**5**) (25.0 mg, 0.0213 mmol) and C_{60} (16.0 mg, 0.0220 mmol) contained in a 100 mL three-neck flask equipped with a reflux condenser was heated to reflux for 1 h. The reaction mixture changed from purple to dark brown, and a new set of peaks corresponding to **1** developed in the IR (ν_{CO}) spectrum. The solvent was removed under vacuum, and the dark residue was separated on a silica gel TLC plate (CS_2) to give C_{60} (2.9 mg, 0.0040 mmol, 18% recovery), **1** (8.2 mg, 0.0045 mmol, 21% based on **5**)), and **5** (4.3 mg, 0.0037 mmol, 17% recovery) in order of elution.

Preparation of $Ru_5C(CO)_{10}(\mu\text{-}\eta^1,\eta^1\text{-dppe})(\mu_3\text{-}\eta^2,\eta^2,\eta^2\text{-}C_{60})$ (2). A. A chlorobenzene (30 mL) solution of $Ru_5C(CO)_{15}$ (40.0 mg, 0.0427 mmol) and C_{60} (31.0 mg, 0.0430 mmol) contained in a 100 mL three-neck flask equipped with a reflux condenser was heated to reflux for 1 h. The reaction mixture was cooled to room temperature, 1,2-bis(diphenylphosphino)ethane (dppe) (17.0 mg, 0.0427 mmol) was added, and the reaction mixture was again heated to reflux for 5 min. The reaction mixture was cooled to room temperature, and the solvent was removed under vacuum. The dark residue was separated with carbon disulfide/chloroform (10/1) on a silica gel TLC plate to give unreacted C_{60} (8.5 mg, 0.0118 mmol, 27% recovery) and **2** (11.7 mg, 0.0061 mmol, 14% based on $Ru_5C(CO)_{15}$) in order of elution. Anal. Calcd for $C_{90}H_{15}O_{11}PRu_5 \cdot CH_2Cl_2$: C, 58.81; H, 1.31. Found: C, 58.85; H, 1.17. Negative-ion FAB mass spectrum (^{102}Ru): *m/z* 1920 ($[Ru_5C(CO)_{10}(dppe)(C_{60})]^-$). IR ($CS_2$): ν_{CO} 2035(w), 2011(s), 1990(vw, br), 1983(w, br) cm^{-1}. $^{31}P\{^1H\}$ NMR (162 MHz, 1,2-$C_6H_4Cl_2$/$CDCl_3$ (1/3), 20 °C): δ 48.6 (s).

B. A chlorobenzene (30 mL) solution of $Ru_5C(CO)_{13}(\mu\text{-}\eta^1,\eta^1$-dppe) (**6**) (27.3 mg, 0.0213 mmol) and C_{60} (15.4 mg, 0.0220 mmol) contained in a 100 mL three-neck flask equipped with a reflux condenser was heated to reflux for 1.5 h. The color of the reaction mixture changed from purple to dark brown, and a new set of peaks corresponding to **2** developed in the IR (ν_{CO}) spectrum. The solvent was removed under vacuum, and the dark residue was separated on a silica gel TLC plate (CS_2) to give a trace amount of C_{60} and **2** (11.2 mg, 0.0058 mmol, 27% based on **6**) in order of elution.

Preparation of $Ru_5C(CO)_{11}(\eta^1\text{-dppf})(\mu_3\text{-}\eta^2,\eta^2,\eta^2\text{-}C_{60})$ (3) and $Ru_5C(CO)_{10}(\mu\text{-}\eta^1,\eta^1\text{-dppf})(\mu_3\text{-}\eta^2,\eta^2,\eta^2\text{-}C_{60})$ (4). A. A chlorobenzene (30 mL) solution of $Ru_5C(CO)_{15}$ (80.0 mg, 0.0853 mmol) and C_{60} (61.5 mg, 0.0853 mmol) contained in a 100 mL three-neck flask equipped with a reflux condenser was heated to reflux for 1 h. The reaction mixture was cooled to room temperature, dppf (46.5 mg, 0.0944 mmol) was added, and the reaction mixture was again heated to reflux for 5 min. The reaction mixture was cooled to room temperature, and the solvent was removed under vacuum. The dark residue was separated on a silica gel TLC plate (CS_2) to give unreacted C_{60} (15.1 mg, 0.0210 mmol, 25% recovery), **4** (25.5 mg, 0.0123 mmol, 14% based on $Ru_5C(CO)_{15}$), and **3** (7.2 mg, 0.0034 mmol, 4% based on $Ru_5C(CO)_{15}$) in order of elution. Characterization data for **3**. Anal. Calcd for $C_{106}H_{28}O_{11}P_2FeRu_5$: C, 60.61; H, 1.34. Found: C, 60.67; H, 1.12. Negative-ion FAB mass spectrum (^{102}Ru): *m/z* 2104 ($[Ru_5C(CO)_{11}(dppf)(C_{60})]^-$). IR ($CS_2$): ν_{CO} 2068(s), 2029(s), 2020(s), 2011(s) cm^{-1}. $^{31}P\{^1H\}$ NMR (162 MHz, 1,2-$C_6H_4Cl_2$/$CDCl_3$ (1/3), 20 °C): δ 43.7 (s), −15.9 (s). Characterization data for **4**. Anal. Calcd for $C_{105}H_{28}O_{10}P_2FeRu_5$: C, 60.85; H, 1.36. Found: C, 60.70; H, 1.24. Negative-ion FAB mass spectrum (^{102}Ru): *m/z* 2076 ($[Ru_5C(CO)_{10}(dppf)(C_{60})]^-$) as well as 2076 − 28*x*, $x = 1-2$ ($[Ru_5C(CO)_{10}(dppf)(C_{60})]^- - xCO$). IR ($CS_2$): ν_{CO} 2035(w), 2010(s), 1986(w, br), 1976(w, br) cm^{-1}. $^{31}P\{^1H\}$ NMR (162 MHz, 1,2-$C_6H_4Cl_2$/$CDCl_3$ (1/3), − 60 °C): δ 41.3 (d, $J = 6.5$ Hz), 37.9 (d).

B. A dichloromethane (20 mL) solution of $Ru_5C(CO)_{15}$ (20.0 mg, 0.0213 mmol) was prepared in a 100 mL three-neck flask equipped with a reflux condenser. The ligand dppf (11.9 mg, 0.0242 mmol) was added to the stirred solution against a nitrogen stream. The IR (ν_{CO}) spectrum indicated complete formation of $Ru_5C(CO)_{13}(\mu\text{-}\eta^1,\eta^1$-dppf) (**7**) after 5 min. The solvent was removed under vacuum. Chlorobenzene (30 mL) and C_{60} (15.4 mg, 0.0214 mmol) were introduced to the flask, and the reaction mixture was heated to reflux for 1.5 h. The color of the reaction mixture changed from purple to dark brown, and a new set of peaks corresponding to **4** developed in the IR (ν_{CO}) spectrum. The solvent was removed under vacuum, and the dark residue was separated on a silica gel TLC plate (CS_2) to give C_{60} (2.1 mg, 0.0029 mmol, 14% recovery) and **4** (8.5 mg, 0.0043 mmol, 20% based on $Ru_5C(CO)_{15}$) in order of elution.

Pyrolysis of 3. A chlorobenzene (15 mL) solution of **3** (5.0 mg, 0.0024 mmol) was prepared in a 100 mL three-neck flask equipped with a reflux condenser. The solution was heated to reflux, and the IR (ν_{CO}) spectrum indicated a smooth transformation of **3** into **4** over 1 h. The solvent was removed

(5) Shriver, D. F.; Drezdon, M. A. *The Manipulation of Air-Sensitive Compounds*, 2nd ed.; John Wiley & Sons: New York, 1986.

Table 1. Crystallographic Data for Compounds $Ru_5C(CO)_{11}(PPh_3)(C_{60})$ (1), $Ru_5C(CO)_{10}(dppe)(C_{60})$ (2), $Ru_5C(CO)_{10}(dppf)(C_{60})$ (4), $Ru_5C(CO)_{13}(dppf)$ (7), $PtRu_5C(CO)_{11}(dppe)(C_{60})$ (8), and $PtRu_5C(CO)_{14}(dppe)$ (9)

	1·$5CS_2$	**2**·CH_2Cl_2	**4**·CH_2Cl_2	**7**·$1.5C_6H_6$	**8**·$2CS_2$	**9**
formula	$C_{91.5}H_{15}O_{11}PRu_5S_3$	$C_{98}H_{26}Cl_2O_{10}P_2Ru_5$	$C_{106}H_{30}Cl_2FeO_{10}P_2Ru_5$	$C_{57}H_{37}FeO_{13}P_2Ru_5$	$C_{100}H_{24}O_{11}P_2PtRu_5S_4$	$C_{41}H_{24}O_{14}P_2PtRu_5$
fw	1922.54	2001.38	2157.34	1553.01	2291.81	1502.98
cryst syst	triclinic	monoclinic	monoclinic	triclinic	triclinic	monoclinic
space group	$P\bar{1}$	$P2_1/n$	$P2_1$	$P\bar{1}$	$P\bar{1}$	$P2_1/n$
a (Å)	10.009(1)	16.697(1)	13.5677(4)	11.082(1)	12.018(1)	14.596(1)
b (Å)	13.389(1)	16.759(1)	17.7866(6)	13.215(1)	16.234(1)	19.693(1)
c (Å)	26.951(1)	24.794(2)	16.7473(6)	20.375(1)	21.260(1)	15.693(1)
α (deg)	77.552(1)	90	90	96.574(1)	67.780(1)	90
β (deg)	80.590(1)	90.88(1)	92.362(1)	102.096(1)	74.277(1)	99.431(1)
γ (deg)	70.210(1)	90	90	106.385(1)	77.090(1)	90
V(Å^3)	3302.26(7)	6937.0(7)	4038.1(2)	2750.6(3)	3662.14(9)	4449.77(7)
Z	2	4	2	2	2	4
ρ_c (g cm^{-3})	1.933	1.916	1.774	1.875	2.078	2.243
μ(cm^{-1})	1.310	1.260	1.259	1.717	3.139	4.923
R_{int}	0.0473	0.1992	0.1235	0.0628	0.0926	0.0630
R_1[a]	0.0695	0.1305	0.1019	0.0578	0.0439	0.0392
wR_2[b]	0.1706	0.2263	0.2360	0.1091	0.1206	0.0752

[a] $R_1 = \Sigma||F_o| - |F_c||/\Sigma|F_o|$. [b] $wR_2 = \{\Sigma[w(F_o^2 - F_c^2)^2]/\Sigma w(F_o^2)^2]\}^{1/2}$.

under vacuum, and the dark residue dissolved in carbon disulfide was eluted on a silica gel TLC plate to give **4** (1.7 mg, 0.0008 mmol, 33%) and a trace amount of **3** in order of elution.

Preparation of $Ru_5C(CO)_{13}(\mu\text{-}\eta^1,\eta^1\text{-dppf})$ (7). A dichloromethane (20 mL) solution of $Ru_5C(CO)_{15}$ (43.0 mg, 0.0459 mmol) was prepared in 100 mL Schlenk tube. The ligand dppf (25.5 mg, 0.0518 mmol) was added as a solid against a nitrogen stream, and the resulting solution was stirred for 5 min. The solution color changed quickly from red to red purple with an accompanying change of the IR signals to 2072(m), 2037(m), 2024(s), 2002(m), and 1995(m, sh) cm^{-1}. The solvent was removed under vacuum, the residue was washed with hexane (ca. 20 mL), and the resulting dark purple solid (57.5 mg, 0.0400 mmol, 87%) was dried under vacuum. Anal. Calcd for $C_{48}H_{28}O_{13}P_2FeRu_5$: C, 40.26; H, 1.69. Found: C, 40.12; H, 1.65. Negative-ion FAB mass spectrum (^{102}Ru): m/z 1440 ($[Ru_5C(CO)_{13}(dppf)]^-$) as well as 1440 − 28x, x = 1−2 ($[Ru_5C(CO)_{13}(dppf)]^- - xCO$). IR ($CH_2Cl_2$): ν_{CO} 2072(m), 2037(m), 2024(s), 2002(m), 1995(m, sh) cm^{-1}. $^{31}P\{^1H\}$ NMR (162 MHz, $CDCl_3$, 50 °C): δ 28.6 (s, br).

Preparation of $PtRu_5C(CO)_{11}(\eta^2\text{-dppe})(\mu_3\text{-}\eta^2,\eta^2,\eta^2\text{-}C_{60})$ (8). A. A chlorobenzene (30 mL) solution of $PtRu_5C(CO)_{14}$(COD) (40.0 mg, 0.0330 mmol) and C_{60} (26.1 mg, 0.0362 mmol) contained in a 100 mL three-neck flask equipped with a reflux condenser was heated to reflux for 1 h. The IR spectrum developed a completely new set of peaks at 2080(s), 2051(s, sh), 2045(vs), 2030(m), and 2022(m) cm^{-1}, and the color changed from red brown to dark brown. The reaction mixture was cooled to room temperature, dppe (14.5 mg, 0.0364 mmol) was added, and the reaction mixture was again heated to reflux for 5 min. The reaction mixture was cooled to room temperature, and the solvent was removed under vacuum. The dark residue was separated with carbon disulfide/chloroform (10/1) on a silica gel TLC plate to give unreacted C_{60} (5.4 mg, 0.0075 mmol, 21% recovery), **2** (1.5 mg, 0.0008 mmol, 2% based on $PtRu_5C(CO)_{14}$(COD)), and **8** (16.1 mg, 0.0075 mmol, 23% based on $PtRu_5C(CO)_{14}$(COD)) in order of elution. Anal. Calcd for $C_{98}H_{24}O_{11}P_2PtRu_5 \cdot CS_2$: C, 53.66; H, 1.09. Found: C, 53.83; H, 1.18. Negative-ion FAB mass spectrum (^{102}Ru): m/z 2143 ($[PtRu_5C(CO)_{11}(dppe)(C_{60})]^-$), 2115 ($[PtRu_5C(CO)_{11}(dppe)(C_{60})]^-$ − CO). IR (CS_2): ν_{CO} 2046(vs), 2016(vs), 2009(s, sh), 1989(m, br), 1954(w, br)cm^{-1}. $^{31}P\{^1H\}$ NMR (162 MHz, 1,2-$C_6H_4Cl_2$/$CDCl_3$ (1/3), 50 °C): δ 58.0 (t, br, J_{Pt-P} = 3640 Hz).

$PtRu_5C(^{13}CO)_{11}(dppe)(C_{60})$ was prepared from $PtRu_5C(^{13}CO)_{14}$(COD) (ca. 95% ^{13}C). ^{13}C NMR (100 MHz, C_6H_5Cl/CD_2Cl_2 (1/2), 22 °C): δ 203 (s, br).

B. A chlorobenzene (20 mL) solution of $PtRu_5C(CO)_{16}$ (20.0 mg, 0.0172 mmol) and C_{60} (12.5 mg, 0.0173 mmol) contained in a 100 mL three-neck flask equipped with a reflux condenser was heated to reflux for 1 h. The IR spectrum developed new peaks at 2080(m), 2066(m), 2051(m, sh), and 2045(vs) cm^{-1}, and the color changed from red brown to dark brown. The reaction mixture was cooled to room temperature, dppe (6.9 mg, 0.0173 mmol) was added, and the reaction mixture was again heated to reflux for 5 min. The reaction mixture was cooled to room temperature, and the solvent was removed under vacuum. The dark residue was separated with carbon disulfide/chloroform (10/1) on a silica gel TLC plate to give unreacted C_{60} (3.4 mg, 0.0047 mmol, 27% recovery), **2** (1.9 mg, 0.0008 mmol, 5% based on $PtRu_5C(CO)_{16}$), and **8** (2.7 mg, 0.0013 mmol, 7% based on $PtRu_5C(CO)_{16}$) in order of elution.

Preparation of $PtRu_5C(CO)_{14}(\eta^2\text{-dppe})$ (9). A dichloromethane (20 mL) solution of $PtRu_5C(CO)_{14}$(COD) (40.0 mg, 0.0330 mmol) was prepared in a 100 mL Schlenk tube. The ligand dppe (13.2 mg, 0.0331 mmol) was added as a solid against a nitrogen stream, and the resulting solution was stirred for 10 min. The solution color changed quickly from red to red brown with an accompanying change of the IR signals to 2069(w), 2043(vs), and 2011(s, br) cm^{-1}. The solvent was removed under vacuum, the residue was washed with hexane (ca. 10 mL), and the resulting dark purple solid (45.2 mg, 0.0301 mmol, 91%) was dried under vacuum. Anal. Calcd for $C_{41}H_{24}O_{14}P_2PtRu_5$: C, 32.76; H, 1.61. Found: C, 32.36; H, 1.65. Negative-ion FAB mass spectrum (^{102}Ru): m/z 1507 ($[PtRu_5C(CO)_{14}(dppe)]^-$) as well as 1507 − 28$x$, x = 1−3 ($[PtRu_5C(CO)_{14}(dppe)]^- - xCO$). IR ($CH_2Cl_2$): ν_{CO} 2069(w), 2043(vs), 2011(s, br) cm^{-1}. ^{1}H NMR (400 MHz, CD_2Cl_2, 20 °C): δ 7.50−7.40 (m, 20H), 2.54 (m, 4H). $^{31}P\{^1H\}$ NMR (162 MHz, CD_2Cl_2, 20 °C): δ 54.6 (t, J_{Pt-P} = 3840 Hz).

X-ray Crystallography. Crystals of **1**, **2**, and **7** were grown by solvent evaporation at room temperature: from carbon disulfide for **1**, dichloromethane for **2**, and dichloromethane/chlorobenzene for **7**. Crystals of **4** were obtained from dichloromethane/chlorobenzene at −5 °C. The data crystal for **2** was exceptionally small (0.02 × 0.06 × 0.06 mm^3), and that for **4** was very thin (0.01 × 0.09 × 0.15 mm^3). Crystals of **8** and **9** were grown by slow solvent interdiffusion at room temperature: for **8** of heptane into carbon disulfide and for **9** of hexane into dichloromethane. Data collections were carried out at 198(2) K on a Siemens SMART/CCD automated diffractometer. All data processing was performed with the integrated program package SHELXTL.[6] Absorption corrections were semiempirical for **1** and analytical by integration for **2**, **4**, **7**, **8**, and **9**. Selected crystallographic details are listed in Table 1, and full details are provided in the Supporting Information. The structures were solved by direct meth-

(6) Sheldrick, G. M. *SHELXTL PC, Version 5.0*; Siemens Industrial Automation, Inc.: Madison, WI, 1994.

Table 2. Internuclear Distances for the Cluster Cores of Compounds $Ru_5C(CO)_{11}(PPh_3)(C_{60})$ (1), $Ru_5C(CO)_{10}(dppe)(C_{60})$ (2), $Ru_5C(CO)_{10}(dppf)(C_{60})$ (4), $Ru_5C(CO)_{13}(dppf)$ (7), $PtRu_5C(CO)_{11}(dppe)(C_{60})$ (8), and $PtRu_5C(CO)_{14}(dppe)$ (9)

	1	2	4	7	8	9
Ru1−Ru2	2.855(1)	2.808(2)	2.822(4)	2.786(1)	2.8778(7)	2.918(1)
Ru1−Ru3	2.851(1)	2.857(4)	2.896(4)	2.825(1)	2.8344(7)	2.793(1)
Ru1−Ru4	2.828(1)	2.799(4)	2.845(4)	2.800(1)	2.9492(7)	2.845(1)
Ru1−Ru5	2.876(1)	2.895(4)	2.789(4)	2.808(1)	2.8599(7)	2.806(1)
Ru2−Ru3	2.865(1)	2.839(4)	2.823(4)	2.802(1)	3.0465(7)	2.848(1)
Ru2−Ru5	2.885(1)	2.842(4)	2.889(4)	2.883(1)	2.8149(7)	2.914(1)
Ru3−Ru4	2.837(1)	2.892(4)	2.828(4)	2.884(1)	2.8391(7)	2.949(1)
Ru4−Ru5	2.882(1)	2.866(4)	2.958(4)	2.951(1)	2.8617(7)	2.878(1)
Pt1−Ru2					2.9349(5)	2.8946(8)
Pt1−Ru3					2.9863(5)	3.0033(8)
Pt1−Ru4					2.8745(6)	2.9532(8)
Pt1−Ru5					3.1478(6)	3.1214(8)
Ru1−C100	2.13(1)	2.16(4)	2.15(4)	2.16(1)	2.169(6)	2.102(8)
Ru2−C100	2.04(1)	2.02(4)	2.09(3)	2.09(1)	1.981(6)	2.038(8)
Ru3−C100	2.04(1)	1.99(4)	2.08(4)	2.05(1)	2.085(6)	2.093(8)
Ru4−C100	2.03(1)	2.06(4)	2.04(4)	2.05(1)	2.035(6)	2.018(8)
Ru5−C100	2.02(1)	2.04(4)	1.96(4)	2.02(1)	2.093(6)	2.057(8)
Pt1−C100					2.039(6)	2.054(8)

Table 3. Selected Distances for the C_{60} Ligand in Compounds $Ru_5C(CO)_{11}(PPh_3)(C_{60})$ (1), $Ru_5C(CO)_{10}(dppe)(C_{60})$ (2), $Ru_5C(CO)_{10}(dppf)(C_{60})$ (4), and $PtRu_5C(CO)_{11}(dppe)(C_{60})$ (8)

	1	2	4	8
Ru1−C1	2.29(1)	2.31(4)	2.27(3)	2.279(6)
Ru1−C2	2.26(1)	2.26(3)	2.16(3)	2.213(6)
Ru2−C3	2.26(1)	2.27(3)	2.24(3)	2.143(6)
Ru2−C4	2.22(1)	2.22(3)	2.22(3)	2.181(6)
Ru3−C5	2.25(1)	2.33(4)	2.25(3)	2.265(6)
Ru3−C6	2.21(1)	2.25(3)	2.23(3)	2.142(6)
C1−C2	1.42(2)	1.49(5)	1.37(4)	1.437(9)
C2−C3	1.47(2)	1.50(4)	1.52(4)	1.508(8)
C3−C4	1.44(2)	1.37(4)	1.39(4)	1.459(9)
C4−C5	1.48(2)	1.48(4)	1.50(4)	1.474(9)
C5−C6	1.46(2)	1.40(4)	1.48(4)	1.431(9)
C6−C1	1.48(2)	1.40(5)	1.42(4)	1.476(10)

ods.[7] Hydrogen atoms were not included in the final structure factor calculations. The lattice solvent molecules present with **1**, **2**, **4**, **7**, and **8** were refined with fixed distances between the non-hydrogen atoms. All non-hydrogen atoms were refined with anisotropic thermal coefficients for **1**, **7**, **8**, and **9**, and only ruthenium atoms were refined with anisotropic thermal coefficients for **2**. Ruthenium, iron, and phosphorus atoms were refined with anisotropic thermal coefficients for **4**. Successful convergences of full-matrix least-squares refinement based on F^2 were indicated by the maximum shift/error for the final cycle. The final difference Fourier maps had no significant features. The metal−metal distances in the cluster cores of these compounds are shown in Table 2, and the selected distances for the C_{60} ligand in **1**, **2**, **4**, and **8** are presented in Table 3.

Results and Discussion

Synthesis and Characterization of Face-Coordinated C_{60} Complexes. The interaction of $Ru_5C(CO)_{15}$ and C_{60} in hot chlorobenzene forms a brown complex that can be separated by thin-layer chromatography and shows IR (ν_{CO}) peaks at 2087(s), 2060(m), 2038(m), and 2024(vs) cm^{-1}, consistent with the presence of $Ru_5C(CO)_{12}(C_{60})$. However, even though this brown material is mobile on the TLC plate, it becomes extremely insoluble after solvent removal, which precludes further characterization by NMR spectroscopy or X-ray crystallography. Nevertheless, in situ treatment of this initial complex with PPh_3 in hot chlorobenzene, followed by solvent removal under vacuum, provides a new dark brown compound $Ru_5C(CO)_{11}(PPh_3)(C_{60})$ (**1**), which shows moderate solubilities in dichloromethane, carbon disulfide, and chlorobenzene and can be fully purified by TLC (SiO_2/CS_2) and crystallization (CS_2). The yield of **1** is 19% from $Ru_5C(CO)_{15}$ with 33% C_{60} recovered, but no other significant soluble product is observed.

The same synthetic approach can be applied to prepare diphosphine ligand substituted compounds **2**, **3**, and **4**. The interaction of $Ru_5C(CO)_{15}$ with C_{60} in chlorobenzene followed by dppe provides $Ru_5C(CO)_{10}(dppe)(C_{60})$ (**2**). The use of dppf initially forms both the monodentate derivative $Ru_5C(CO)_{11}(\eta^1\text{-dppf})(C_{60})$ (**3**) and the bidentate derivative $Ru_5C(CO)_{10}(dppf)(C_{60})$ (**4**), but extended thermolysis of **3** converts it to **4**. Compounds **1**−**4** are readily formulated on the basis of strong molecular ions in their negative-ion FAB mass spectra. Comparison of solution IR (ν_{CO}) spectra also clearly shows that derivative **3** is structurally related to **1** and that **2** and **4** comprise a separate, analogous pair. Compounds **1**, **2**, and **4** can also be prepared by direct interaction of the substituted clusters $Ru_5C(CO)_{14}(PPh_3)$ (**5**),[3] $Ru_5C(CO)_{13}(dppe)$ (**6**),[3] and $Ru_5C(CO)_{13}(dppf)$ (**7**) with C_{60} in refluxing chlorobenzene. The substituted clusters **5** and **6** were previously known,[3] and **7** is readily prepared from $Ru_5C(CO)_{15}$ and dppf (see Experimental Section). The overall yields of the C_{60} complexes obtained this way (18−27%) are comparable with those obtained by the original procedure. Furthermore, no structural isomers for complexes **1**, **2**, and **4** are observed, which demonstrates the structural specificity of the Ru_5C-C_{60} interaction (vide infra).

The synthesis of a C_{60} complex involving a heterometallic $PtRu_5C$ core can be accomplished by an analogous procedure. The interaction of either $PtRu_5C(CO)_{14}(COD)$[4] or $PtRu_5C(CO)_{16}$[4] and C_{60} in refluxing chlorobenzene affords a red-brown complex that exhibits IR bands at 2080(s), 2051(s, sh), 2045(vs), 2030(m), and 2022(m) cm^{-1}, consistent with the presence of $PtRu_5C(CO)_{13}(C_{60})$. Again, it is necessary to form a derivative for solubility, and in situ treatment of the intermediate with dppe provides the dark brown complex $PtRu_5C(CO)_{11}(dppe)(C_{60})$ (**8**) (23% yield), which can be purified

(7) Sheldrick, G. M. *Acta Crystallogr.* **1990**, *A46*, 467.

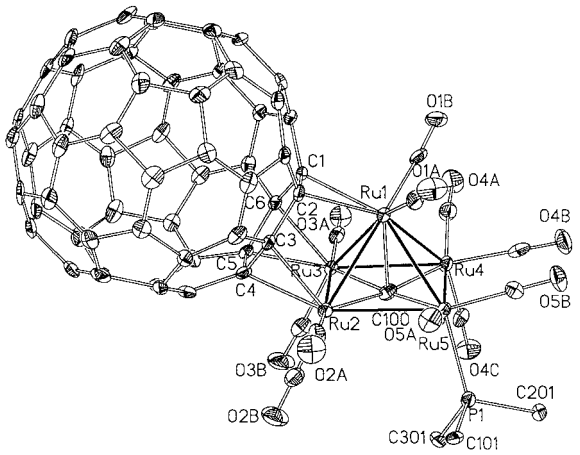

Figure 1. Structural diagram of $Ru_5C(CO)_{11}(PPh_3)(C_{60})$ (**1**) (35% thermal ellipsoids). Phenyl groups have been removed except for the ipso carbons (C101, C201, and C301).

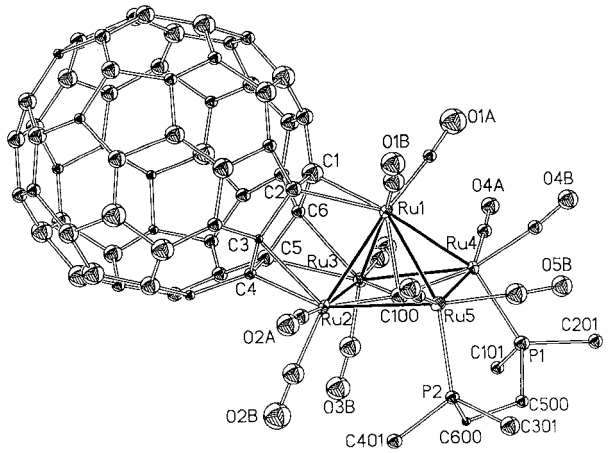

Figure 2. Structural diagram of $Ru_5C(CO)_{10}(dppe)(C_{60})$ (**2**) (35% thermal ellipsoids). Phenyl groups have been removed except for the ipso carbons (C101, C201, C301, and C401).

by TLC (SiO_2/CS_2) and crystallization. Both ^{31}P NMR spectroscopy and X-ray crystallography show that the dppe ligand chelates the platinum center in complex **8** (vide infra). In this case, however, the corresponding substituted cluster $PtRu_5C(CO)_{14}(dppe)$ (**9**) does not react with C_{60} to give **8**.

X-ray Crystallographic Studies. The structural diagrams of **1**, **2**, **4**, **7**, **8**, and **9** are shown in Figures 1−6. The metal−metal distances in the cluster cores of these compounds are shown in Table 2, and selected distances for the C_{60} ligand in **1**, **2**, **4**, and **8** are presented in Table 3.

For compounds **1**, **2**, and **4** involving the Ru_5C framework, the C_{60} ligand is bound in a μ_3-η^2,η^2,η^2 fashion on one triangular face of the square-pyramidal Ru_5C framework. In **1**, the PPh_3 ligand is located in an axial position on one of the basal ruthenium atoms not bonded to the C_{60} ligand. In **2** and **4**, the diphosphine ligand (dppe or dppf) bridges the two axial positions on the basal ruthenium atoms not bonded to the C_{60} ligand. All carbonyl ligands in each compound are terminal.

The carbon−carbon distances in the C_6 ring of C_{60} bound to the metal framework in **1** alternate in length (average 1.44 and 1.48 Å, respectively), and the Ru−C distances in **1** also alternate in length (average 2.23 and 2.27 Å, respectively), resulting in a slight twist of the Ru_3 triangle with respect to the C_6 ring. The face-capping bonding mode was also seen for the benzene derivative $Ru_5C(CO)_{12}(\mu_3$-η^2,η^2,η^2-$C_6H_6)$, and similar bond length alternations in the benzene ring (average 1.36 and 1.44 Å, respectively) and in the Ru−C distances (average 2.23 and 2.29 Å, respectively) were

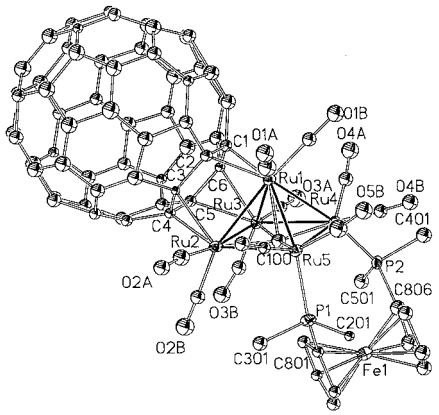

Figure 3. Structural diagram of $Ru_5C(CO)_{10}(dppf)(C_{60})$ (**4**) (35% thermal ellipsoids). Phenyl groups have been removed except for the ipso carbons (C201, C301, C401, and C501).

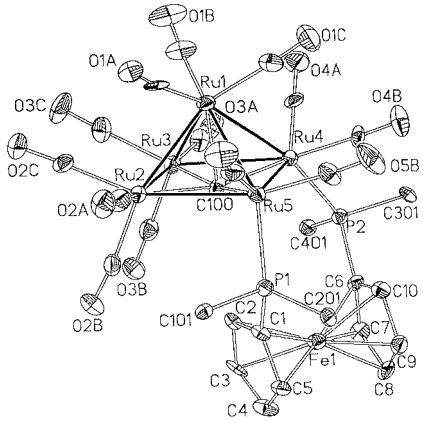

Figure 4. Structural diagram of $Ru_5C(CO)_{13}(dppf)$ (**7**) (35% thermal ellipsoids). Phenyl groups have been removed except for the ipso carbons (C101, C201, C301, and C401).

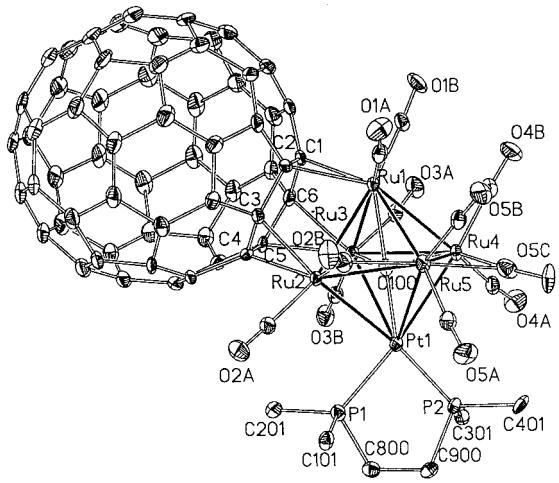

Figure 5. Structural diagram of $PtRu_5C(CO)_{11}(dppe)(C_{60})$ (**8**) (35% thermal ellipsoids). Phenyl groups have been removed except for the ipso carbons (C101, C201, C301, and C401).

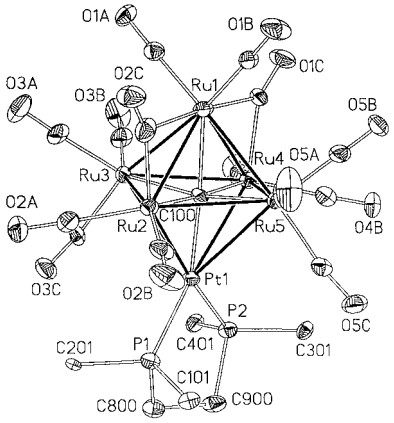

Figure 6. Structural diagram of $PtRu_5C(CO)_{14}(dppe)$ (**9**) (35% thermal ellipsoids). Phenyl groups have been removed except for the ipso carbons (C101, C201, C301, and C401).

determined.[8] A detailed description of Ru−C interactions or C−C distances of the C_6 ring bound to the metal framework for **2** and **4** is not feasible due to the limited quality of the solved structures.

The Ru_{basal}−Ru_{basal} distances (average 2.884 Å) of the C_{60} complex **1** associated with the PPh_3-substituted ruthenium are longer than the other two Ru_{basal}−Ru_{basal} distances (average 2.851 Å). In the other PPh_3-substituted compound, **5**, the Ru_{basal}−Ru_{basal} distances (average 2.92 Å) associated with the PPh_3-substituted rutheniums are also longer than the other two Ru_{basal}−Ru_{basal} distances (average 2.82 Å).[3] The distance (2.958(4) Å) between basal rutheniums of **4** bridged by the dppf ligand is notably longer than the other basal−basal Ru−Ru distances (2.823(4), 2.828(4), and 2.889(4) Å). In compound **2**, however, the distance (2.866(4) Å) between the two basal rutheniums bridged by the dppe ligand is similar to other Ru_{basal}−Ru_{basal} distances (2.839(4), 2.842(4), and 2.892(4) Å).

In compound **7**, the dppf ligand connects two axial positions in bridging two basal ruthenium atoms as in **4**. Compound **6**, similarly prepared from the interaction between $Ru_5C(CO)_{15}$ and dppe at room temperature, has a very similar IR spectrum (ν_{CO} 2072(m), 2036(m), 2023(s), 2005(m), and 1997(m, sh) cm^{-1}) to that of **7**. Thus, the same structural motif featuring a bridging dppe ligand is expected for **6**. This is in contrast with the previously proposed structure involving a chelating ligand;[3] however, this conclusion was based primarily on the structure of the product resulting from the reaction of **6** with dihydrogen under severe conditions. The distance (2.951(1) Å) between basal rutheniums of **7** bridged by the dppf ligand is notably longer than the other basal Ru−Ru distances (2.802(1), 2.883(1), and 2.884(1) Å) as in **4**. Also, the Ru_{basal}−Ru_{basal} distances (average 2.884 Å) associated with one phosphine-substituted ruthenium are longer than the Ru_{basal}−Ru_{basal} distance (2.802(1) Å) not associated with phosphine-substituted rutheniums. In the related compound $Ru_6C(CO)_{15}(\mu\text{-}\eta^1,\eta^1\text{-dppf})$,[9] the initial closo octahedral framework is opened upon coordination of the dppf ligand to give a hinged square pyramid, which shows two very long Ru−Ru distances, 3.450(1) and 3.171(1) Å, associated with the bridging dppf ligand.

Overall, the Ru−Ru distances in the cluster faces associated with the C_6 ring of the C_{60} ligand are elongated relative to those in analogous non-C_{60} compounds, demonstrating the steric requirements of a C_{60} ligand replacing three carbonyl ligands. The Ru−Ru distances (average 2.857 Å) associated with the C_6 ring of the C_{60} ligand in **1** are ca. 0.04 Å longer than the Ru−Ru distances in the two Ru_3 triangles of **5** (average 2.811 and 2.820 Å) not associated with the PPh_3-substituted Ru atom.[3] Also, a similar elongation is observed in the C_{60}-coordinated Ru−Ru distances (average 2.834 and 2.847 Å, respectively) in **2** and **4** as compared to the Ru−Ru distances (average 2.804 Å) in the Ru_3 triangle of **7** not associated with the dppf ligand. For comparison, no such elongation was observed for the benzene adduct $Ru_5C(CO)_{12}(\mu_3\text{-}\eta^2,\eta^2,\eta^2\text{-}C_6H_6)$.[8] The Ru_{apical}−$C_{carbide}$, Ru_{basal}−$C_{carbide}$, and Ru−P distances in the C_{60} substituted complexes (2.12(1), average 2.03, and 2.35(1) Å for **1**; 2.16(4), average 2.03, and average 2.31 Å for **2**; 2.15(4), average 2.04, and average 2.34 Å for **4**) are all similar to those in the non-C_{60} compounds (2.12(1), average 2.04, and 2.38(1) Å for **5** and 2.16(1), average 2.05, and average 2.36 Å for **7**).[3]

The metal framework of **8** is an octahedron as in $PtRu_5C(CO)_{16}$,[4] and the C_{60} ligand is facially coordinated to one Ru_3 triangle. The diphosphine ligand is positioned on the platinum atom as a chelating ligand, and all carbonyl ligands but two are terminal. Two bridging carbonyls are positioned along the Ru2−Ru5 and Ru4−Ru5 edges. The Ru_{apical}−Ru_{basal} distances of **8** alternate in length (average 2.847 and 2.912 Å, respectively), and the Pt−Ru_{basal} distances also alternate in length (average 2.905 and 3.067 Å, respectively) as in $PtRu_5C(CO)_{16}$ (average 2.821 and 2.938 Å for the Ru_{apical}−Ru_{basal}; average 2.830 and 2.994 Å for Pt−Ru_{basal}).[4] The Pt−Ru_{basal} distances of **8** are longer than the counterparts in $PtRu_5C(CO)_{16}$, consistent with the presence of a dppe ligand that is sterically more demanding than two carbonyl ligands.[4]

Compound **9** also displays an octahedral $PtRu_5C$ cluster core, and the diphosphine ligand again is positioned on the platinum atom as a chelating ligand. All carbonyl ligands but two are terminal. The two bridging carbonyls are positioned along the Ru1−Ru2 and Ru1−Ru4 edges. The molecule exhibits approximate C_{2v} symmetry with the C_2 axis bisecting the ethylene backbone of the dppe ligand. The Ru_{apical}−Ru_{basal} distances of **9** alternate in length (average 2.800 and 2.882 Å, respectively), and the Pt−Ru_{basal} distances also alternate in length (average 2.924 and 3.062 Å, respectively) as in $PtRu_5C(CO)_{16}$ and **8**. Overall, the Pt−Ru_{basal} distances of **9** are longer and the Ru_{apical}−Ru_{basal} distances of **9** are shorter than the counterparts in $PtRu_5C(CO)_{16}$, which again can be attributed to the steric requirement of the dppe ligand.

The carbon−carbon distances in the C_6 ring of C_{60} bound to the metal framework in **8** alternate in length (average 1.44 and 1.49 Å, respectively), whereas the

(8) (a) Bailey, P. J.; Braga, D.; Dyson, P. J.; Grepioni, F.; Johnson, B, F. G.; Lewis, J.; Sabatino, P. *J. Chem. Soc., Chem. Commun.* **1992**, 177. (b) Braga, D.; Grepioni, F.; Sabatino, P.; Dyson, P. J.; Johnson, B. F. G.; Lewis, J.; Bailey, P. J.; Raithby, P. R.; Stalke, D. *J. Chem. Soc., Dalton Trans.* **1993**, 985.

(9) Blake, A. J.; Harrison, A.; Johnson, B. F. G.; McInnes, E. J. L.; Parsons, S.; Shephard, D. S.; Yellowlees, L. J. *Organometallics* **1995**, *14*, 3160.

Scheme 2

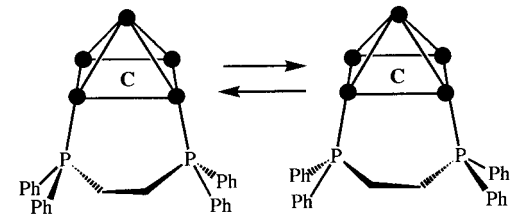

2

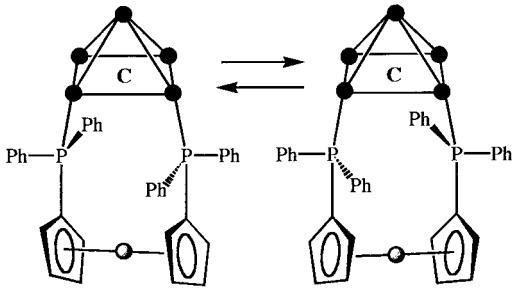

4 or **7**

Ru−C interactions do not alternate in length. The Ru−Ru distances (average 2.920 Å) associated with the C_6 ring of the C_{60} ligand in **8** are lengthened from the Ru−Ru distances (average 2.843, 2.853, 2.862, and 2.879 Å, respectively) in the four Ru_3 triangles of **9**.[4] Accordingly, the $Ru_{apical}-C_{carbide}$ distance (2.17(1) Å) of **8** is a little longer than that (2.10(1) Å) of **9**. However, the $Ru_{basal}-C_{carbide}$, $Pt-C_{carbide}$, and Pt−P distances (average 2.06, 2.04(1), and average 2.28 Å) of the C_{60}-substituted **8** are all similar to those of **9** (average 2.05, 2.05(1), and 2.28 Å).

Solution NMR Spectroscopic Studies. The ^{31}P NMR spectrum of **1** shows a singlet at δ 47.3. In the ^{13}C NMR spectrum of ^{13}CO-enriched **1**, nine peaks with relative intensities of 1:1:1:1:1:1:3:1:1 are observed in the carbonyl region. The signal with intensity three is interpreted to result from rapid three-fold rotation of the three carbonyls on the unsubstituted basal ruthenium atom, Ru4. Thus, the signal patterns in the solution ^{31}P and ^{13}C NMR spectra are consistent with the solid-state structure.

In the solid-state structure of **2**, the two phosphorus atoms are inequivalent. However, the ^{31}P NMR spectrum of compound **2** at room temperature exhibits only one sharp signal at δ 48.6, indicating the presence of an effective mirror plane bisecting the C_{60} ligand as well as the Ru−Ru bond bridged by the dppe ligand. This suggests relatively rapid inversion of the ethylene unit linking the two phosphorus atoms as shown in Scheme 2.

The ^{31}P NMR spectrum of the η^1-dppf compound **3** shows two signals at δ 43.7 and −15.9 for the two inequivalent phosphorus atoms, one coordinated and one uncoordinated, respectively. For the bridging dppf compound **4**, two ^{31}P NMR signals at δ 41.3 and 37.9 are observed at −60 °C, corresponding to the two inequivalent phosphorus atoms of the dppe ligand expected from the solid-state structure. These two signals coalesce to one signal at higher temperatures (T_c = 273 K). The ^{31}P NMR spectrum of **7** at 50 °C shows one broad signal for the two phosphorus atoms, which again are inequivalent in the solid-state structure. These exchange processes in compounds **4** and **7** also indicate the presence of ring inversions involving the bridging ferrocene unit as shown in Scheme 2.

The ^{31}P NMR spectrum of compound **8** at 50 °C exhibits one broad signal at δ 58.0 accompanied by two satellite peaks (J_{Pt-P} = 3640 Hz), again indicating a slow interchange process of the two phosphorus atoms of the dppe ligand, which are inequivalent in the solid-state structure. This generation of an effective mirror plane bisecting the C_{60} ligand requires rotation of the dppe ligand on the platinum atom as well as a facile carbonyl scrambling on the Ru_5C framework. Consistent with this interpretation, the ^{13}C NMR spectrum of ^{13}CO-enriched **8** at room temperature exhibits only a broad signal at δ 203, indicating global carbonyl scrambling. The ^{31}P NMR spectrum of compound **9** exhibits one signal at δ 54.6 accompanied by two satellite peaks (J_{Pt-P} = 3840 Hz) for the two phosphorus nuclei of the dppe ligand, consistent with the solid-state structure.

Conclusion

Compounds displaying coordination of C_{60} to a triangular face of the square-pyramidal Ru_5C or octahedral $PtRu_5C$ frameworks can be prepared by the interaction of C_{60} with $Ru_5C(CO)_{15}$ or $PtRu_5C(CO)_{14}(L)$ (L = 2CO or COD) followed by phosphines. The fact that the proposed intermediates, $Ru_5C(CO)_{12}(\mu_3\text{-}\eta^2,\eta^2,\eta^2\text{-}C_{60})$ and $PtRu_5C(CO)_{13}(\mu_3\text{-}\eta^2,\eta^2,\eta^2\text{-}C_{60})$, can undergo a substitution reaction by phosphine ligands under severe conditions reveals the robust nature of the $C_{60}-Ru_5C$ and $C_{60}-PtRu_5C$ bonding. The structural specificity of the $C_{60}-Ru_5C$ cluster interaction is indicated by the observation that compound $Ru_5C(CO)_x(L)(\mu_3\text{-}\eta^2,\eta^2,\eta^2\text{-}C_{60})$ (L = PPh_3, dppe, dppf) can also be prepared from the direct interaction of C_{60} and $Ru_5C(CO)_y(L)$.

Acknowledgment. This material is based upon work supported by the National Science Foundation (Award No. CHE 9414217) and by the Office of Naval Research (Award No. N00014-96-1-0494). Purchase of the Siemens Platform/CCD diffractometer by the School of Chemical Sciences at the University of Illinois was supported by National Science Foundation Grant CHE 9503145. We thank Dr. Scott R. Wilson for X-ray data collection. NMR spectra were obtained using instruments in the Varian Oxford Instrument Center for Excellence in NMR Laboratory in the School of Chemical Sciences; external funding for this instrumentation was obtained from the Keck Foundation, NIH, and NSF.

Supporting Information Available: Tables of positional parameters, bond distances, bond angles, and anisotropic thermal parameters for the structural analysis for **1**, **2**, **4**, **7**, **8**, and **9** (73 pages). Ordering information is given on any current masthead page.

OM971091K